

Thermodynamic Circuits II: Nonequilibrium conductance matrix for a thermoelectric converter

Paul Raux,^{1,2} Christophe Goupil,² and Gatién Verley¹

¹*Université Paris-Saclay, CNRS/IN2P3, IJCLab, 91405 Orsay, France*

²*Université Paris Cité, CNRS, LIED, F-75013 Paris, France*

(Dated: May 21, 2024)

Starting from a linear flux-force relation of a thermoelectric material in local equilibrium, we derive non-linear relations between the currents and forces of a thermoelectric converter (TEC) driven far from equilibrium. Our investigation focuses on a one-dimensional TEC of finite thickness. Building on the achievements of the first paper of this series, we unveil the conservation laws governing physical currents (ie linearly dependent currents). Using the latter allows to put forward two relevant bases of physical and fundamental currents. For these bases, we introduce the concept of non equilibrium conductance matrix to describe the current-force relations of a TEC. This concept will be at the core of the third paper of this series in which we illustrate the serial and parallel association on composite TECs. Finally, we determine in a unified way the optimal working points of the TEC in its two operating modes: the electric generator and the heat pump.

I. INTRODUCTION

In 1931, Lars Onsager proposed his close-to-equilibrium thermodynamics framework [1] leading to intense work aiming at discovering the principles of this new field [2–5]. Thermoelectric materials have long been regarded as paradigmatic systems in the study of the out of equilibrium conversion of heat into electricity. Indeed, in 1948, Callen proposed a concise model for the description of TEC requiring only three parameters called thermoelectric coefficients. This simple model allowed for an analytical study of the energy and matter transport as well as their coupling. At the mesoscopic scale, these parameters are assumed to remain constant irrespective of thermodynamic forces, an assumption leading to the Constant Property Model (CPM). This modeling approach was extended in 1959 for thermoelectric material of macroscopic thickness by A. Ioffe to incorporate dissipative terms and explicit entropy balances with thermostats [6].

Although the CPM approach has been highly successful and is still prevalent today, it faces credibility challenges for macroscopic thermoelectric materials where thermodynamic forces exert significant influence. To circumvent this, thermoelectric materials are often discretized into sections, each assumed to follow the CPM. However, for this method to be operational, one must first understand how the matter and energy transport impedances couple at the interface between CPMs of different thermoelectric coefficients. Indeed, in general, macroscopic TECs have space or force-dependent thermoelectric coefficients. This interface problem led in particular to the concept of relative current [7, 8] which highlights the challenge of optimally coupling two thermodynamic converters.

Except in cases of strong coupling, where energy is entirely conveyed by matter transport, the transport impedances equivalent to the whole discretized TEC are

in general non-linear forms of the impedances of each slice of material and the forces at the boundary of each slice. This complexity often resists simplification, posing challenges for the networking of TECs. This nonlinearity is a general issue in thermodynamic conversion developments when internal parameters become dependent on thermodynamic forces at a global scale. In such scenarios, identifying space-invariant quantities for the out-of-equilibrium system facilitates the system’s description since it reduces the number of degrees of freedom by taking matter and energy conservation into account. For a given CPM describing a TEC, we show that energy and matter fluxes both derive from potentials. Charge and energy conservation then implies that the gradients of these potentials are two space-invariant quantities. This constitutes our first result. The second result of our work is to exhibit conductance matrices accurately defined across various current basis choices thereby preparing the TEC associations (serial and parallel) studied in the third paper of this series to illustrate the results of [9]. This conductance is the matrix analogous to the scalar conductance in stationary electronics.

The initial section of this article showcases how a global-scale framework in thermoelectrics unveils space invariants quantities such as the F functions which characterizes the free fraction of energy in the CPM. Subsequent sections delve into the construction of the nonlinear conductance matrix (section III) and the optimization of the TEG across various operating regimes of electric power generation and heat pump systems (section IV).

II. FROM LOCAL FLUXES TO GLOBAL CURRENTS

In this section, we start from the local description of a TEC in terms of a flux-force characteristics defined by the Onsager matrix and its associated thermoelectric coefficients. Using the conservation of matter and energy

fluxes across a surface \mathcal{A} of a thermoelectric material of finite thickness Δx , we obtain the global current-force characteristic. As compared to Ref. [10], our derivation emphasizes that both charge and energy currents derive from potential functions that we identify. We also shed light on the role of a space independent quantity that we denote F . Finally, we rephrase Domenicali's equation as a necessary condition for the conservation of energy.

A. Local Onsager flux-force relation

In a thermoelectric material, the heat flux \mathbf{J}_Q ($W.m^{-2}$) and the electrical flux \mathbf{J}_C ($C.s^{-1}.m^{-2}$) are coupled through the following flux-force relation:

$$\begin{pmatrix} \mathbf{J}_Q \\ \mathbf{J}_C \end{pmatrix} = \mathbf{L} \begin{pmatrix} -\nabla T \\ \mathcal{E} \end{pmatrix}, \quad (1)$$

where the thermodynamic forces are $\mathcal{E} = -\nabla V$ for the electrical field and ∇T for the temperature gradient. The temperature $T = T(x)$ and the electric potential $V = V(x)$ are assumed to be constant in any transverse plane of the material with constant x value. The response matrix appearing in Eq. (1) is

$$\mathbf{L} = \begin{bmatrix} \alpha^2 \sigma_T T + \kappa_J & \alpha \sigma_T T \\ \alpha \sigma_T & \sigma_T \end{bmatrix}. \quad (2)$$

Due to the fact that the forces and fluxes are not thermodynamically conjugated, the Onsager reciprocity relation does not hold and \mathbf{L} is not symmetric. To recover this symmetry, one should use instead the force vector $(\nabla(\frac{1}{T}), \frac{\mathcal{E}}{T})$ that is conjugated to $(\mathbf{J}_Q, \mathbf{J}_C)$. The transport of heat and electric charge described by Eq. (1) can be interpreted as follows. We recover Fourier's law $\mathbf{J}_Q = -\kappa_J \nabla T$ by taking $\alpha \rightarrow 0$ in the first row of Eq. (1), where κ_J is the thermal conductivity under zero electrical current. In the same limit, we recover Ohm's law $\mathbf{J}_C = \sigma_T \mathcal{E}$, with σ_T the isothermal electrical conductivity. Finally, α is the Seebeck coefficient defined by

$$\alpha = \left. \frac{|\mathcal{E}|}{|\nabla T|} \right|_{\mathbf{J}_C=0} \quad (3)$$

that couples heat and charge fluxes.

The current, i.e. the integrated flux across any plane with constant x value, of electric charge is x independent but not the heat current. To integrate the local flux-force relation and obtain the non-linear current-force characteristic for a finite thickness of thermoelectric material, it is convenient to use the conserved fluxes $(\mathbf{J}_E, \mathbf{J}_C)$ where \mathbf{J}_E is the energy flux defined according to the first law of thermodynamics by

$$\mathbf{J}_E = \mathbf{J}_Q + V(x)\mathbf{J}_C \quad (4)$$

where $V(x)\mathbf{J}_C$ is the flux of electric power crossing the orientated surface \mathcal{A} in the direction of abscissa x . The

vector of forces conjugated to the vector of conserved fluxes is $(\nabla \frac{1}{T}, -\nabla \frac{V}{T})$. The associated flux-force relation reads

$$\begin{pmatrix} \mathbf{J}_E \\ \mathbf{J}_C \end{pmatrix} = \mathcal{L} \begin{pmatrix} \nabla \frac{1}{T} \\ -\nabla \frac{V}{T} \end{pmatrix}, \quad (5)$$

involving the symmetric response matrix

$$\mathcal{L} = \begin{bmatrix} \kappa_J T^2 + T \sigma_T (\alpha T + V)^2 & T \sigma_T (\alpha T + V) \\ T \sigma_T (\alpha T + V) & T \sigma_T \end{bmatrix}. \quad (6)$$

This matrix follows from first using in Eqs. (1-2) the following change of variables

$$\begin{pmatrix} -\nabla T \\ -\nabla V \end{pmatrix} = \begin{bmatrix} 0 & T^2 \\ VT & T \end{bmatrix} \begin{pmatrix} \nabla \frac{1}{T} \\ -\nabla \frac{V}{T} \end{pmatrix}, \quad (7)$$

and second by using Eq. (4) to switch from the vector of heat and charge fluxes to the vector of energy and charge fluxes. In the following, we call Eq. (5) the local flux-force relation for the conserved fluxes. Since we use variables that are conjugated when considering an entropy balance, the matrix \mathcal{L} is symmetric. It is also x dependent via the local temperature T and electric potential V .

B. Current-force relation from integrated fluxes

In this section, we provide the global current-force relation of the TEC of finite thickness Δx subjected to the (Dirichlet) boundary conditions:

$$T(0) = T_l, \quad V(0) = V_l, \quad (8)$$

$$T(\Delta x) = T_r, \quad V(\Delta x) = V_r. \quad (9)$$

Without loss of generality, we assume $T_l > T_r$. We start by showing that both matter and energy fluxes derive from a potential. Using this property, the global current-force relation is then obtained by integrating the differential equations for those potentials on a finite thickness of thermoelectric material. We call TEC the device described by this global current-force relation. We then determine the temperature and electric potential profile in the x direction.

1. Electric current

We start by determining the electric current as a function of the temperature difference $\Delta T = T_r - T_l$ and the tension $\Delta V = V_r - V_l$ between the right and left planes of the TEC. According to Eqs. (1-2), the electric flux \mathbf{J}_C derives from a potential $\varphi(x)$ as

$$\mathbf{J}_C = -\sigma_T \nabla \varphi. \quad (10)$$

where

$$\varphi = \alpha T + V \quad (11)$$

In the stationary state, this flux is divergence less to ensure charge conservation

$$\nabla \cdot \mathbf{J}_C = -\sigma_T \nabla^2 \varphi = 0 \quad (12)$$

From this last equation, we identify the following space independent quantity:

$$\nabla (\alpha T + V) = \text{Constant}. \quad (13)$$

In other words, φ is an affine function of x with coefficients yet to be determined. For our effectively one dimensional TEC under the boundary conditions of Eqs. (8–9), see Fig.1, the solution of Eq. (12) reads

$$\varphi(x) = (\varphi_r - \varphi_l) \frac{x}{\Delta x} + \varphi_l \quad (14)$$

where we have denoted $\varphi_\chi = \alpha T_\chi + V_\chi$ with $\chi = l, r$. Then, the electric current across the oriented surface vector \mathcal{A} follows from the expression of the electric flux (10) combined with Eq.(14) as

$$I_C \equiv \mathbf{J}_C \cdot \mathcal{A} = \frac{\varphi_l - \varphi_r}{R} \quad (15)$$

where we have introduced the electric resistance (analogous to the internal resistance of a Thevenin electric generator)

$$R \equiv \frac{\Delta x}{\sigma_T |\mathcal{A}|}. \quad (16)$$

Remarkably, the expression of I_C given in Eq. (15) takes the form of the Ohm's law generalized to the composite potential φ which encapsulates the coupling between energy and charge transport. φ can then be expressed in term of the thermoelectric coefficients of the TEC and of the potential of the reservoirs as:

$$\varphi(x) = (\alpha \Delta T + \Delta V) \frac{x}{\Delta x} + \alpha T_l + V_l. \quad (17)$$

Then, a second expression of the electrical current follows as

$$I_C = -\frac{1}{R} (\alpha \Delta T + \Delta V) \quad (18)$$

We emphasize that in generator convention a positive power is generated by the TEC and absorbed by the load when $I_C \Delta V > 0$ (for ΔV and I_C aligned in generator convention and anti-aligned in load convention).

2. Energy current

We continue with the determination of the energy current as a function of ΔT and ΔV . According to Eqs. (1–2), the heat flux writes

$$\mathbf{J}_Q = \alpha T \mathbf{J}_C - \kappa_J \nabla T \quad (19)$$

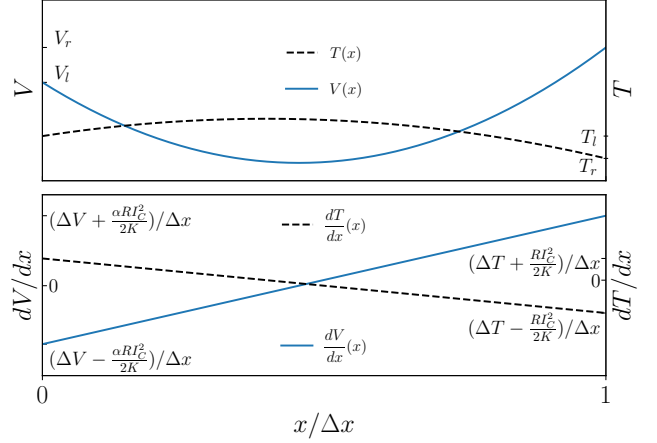


FIG. 1. Electric potential and temperature profile (Top panel) and gradients (Bottom panel) along the x axis of the thermoelectric material under the fixed boundary conditions of Eqs. (8–9). The left vertical axis is for electric potential V profile (respectively gradients) in blue solid line. The right vertical axis is for temperature profile (respectively gradients) in black dashed line.

that, when combined with Eq. (4) and the definition of φ Eq. (11), leads to the energy flux

$$\mathbf{J}_E = \varphi \mathbf{J}_C - \kappa_J \nabla T. \quad (20)$$

We show that \mathbf{J}_E derives from a potential. Indeed, combining Eq. (10) and Eq. (20) yields

$$\mathbf{J}_E = -\kappa_J \nabla \Phi. \quad (21)$$

where

$$\Phi = T + \frac{\sigma_T}{2\kappa_J} \varphi^2 \quad (22)$$

The potential function Φ depends on x through T and φ . Energy conservation is thus ensured if and only if

$$\nabla \cdot \mathbf{J}_E = 0 = -\kappa_J \nabla^2 \Phi \quad (23)$$

This last equation is readily solved as

$$\Phi(x) = (\Phi_r - \Phi_l) \frac{x}{\Delta x} + \Phi_l \quad (24)$$

where we have denoted $\Phi_\chi = T_\chi + \frac{\varphi_\chi^2}{2\kappa_J R}$ with $\chi = l, r$ and introduced the thermal conductivity under zero electric current for the TEC as

$$K \equiv \frac{\kappa_J |\mathcal{A}|}{\Delta x}. \quad (25)$$

The energy current across the oriented surface vector \mathcal{A} then follows from the expression of the energy flux Eq. (21) combined with Eq. (24)

$$I_E \equiv \mathbf{J}_E \cdot \mathcal{A} = K (\Phi_l - \Phi_r) \quad (26)$$

Once again, we remark that the expression of I_E given in Eq. (26) takes a Fourier's law form with thermal resistance $1/K$ and generalized to the composite potential Φ which also encapsulates the coupling between charge and energy transport. We can finally express Φ in term of the thermoelectric coefficients and the potentials of the reservoirs as

$$\Phi(x) = \left(\Delta T - \frac{F}{K} I_C \right) \frac{x}{\Delta x} + T_l + \frac{(\alpha T_l + V_l)^2}{2KR} \quad (27)$$

where we have introduced F which reads

$$F = \frac{\varphi_l + \varphi_r}{2} = \alpha \bar{T} + \bar{V}, \quad (28)$$

the average temperature $\bar{T} = (T_l + T_r)/2$ and the electric potential $\bar{V} = (V_l + V_r)/2$. The energy current can thus be rewritten as

$$I_E = -K\Delta T + F I_C \quad (29)$$

Interestingly, F can be expressed in terms of the charge current by using Eq. (18)

$$F = \varphi_l - \frac{R I_C}{2}, \quad (30)$$

$$F = \varphi_r + \frac{R I_C}{2}. \quad (31)$$

As previously mentioned, in the absence of any leakage term, that is when $K = 0$, the matter and energy currents are strictly proportional. Hence, the parameter F indeed characterizes the free fraction of transported energy. Eqs. (18,29) constitute the integrated current-force characteristics of a TEC where the forces are the temperature and electric potential differences. Section III summarizes these results into the so-called non-equilibrium conductance matrix.

C. Temperature and electric potential profile

We now derive the temperature and the electric potential profile along the x direction of the TEC. The temperature is the solution of Domenicalli's equation [10]. Within our formalism, Domenicalli's equation is in fact equivalent to ensuring the conservation of the total energy flux \mathbf{J}_E in Eq. (20). Indeed, the total energy flux is conserved if it is divergence less $\nabla \cdot \mathbf{J}_E = \mathbf{0}$ which using Eq. (20) reads

$$0 = \nabla (\alpha T + V) \cdot \mathbf{J}_C + (\alpha T + V) \nabla \cdot \mathbf{J}_C - \kappa_J \nabla^2 T \quad (32)$$

Then inserting the charge conservation Eq. (12) in this last equation and solving for $\nabla^2 T$ yields Domenicalli's equation as

$$\nabla^2 T = -\frac{\mathbf{J}_C^2}{\kappa_J \sigma_T}. \quad (33)$$

This equation combined with Eq. (12) gives a similar second order differential equation for the electric potential instead of the temperature

$$\nabla^2 V = \frac{\alpha \mathbf{J}_C^2}{\kappa_J \sigma_T}. \quad (34)$$

For our effectively one dimensional TEC under the boundary conditions of Eqs. (8-9), the temperature and electric potential read

$$T = T_l + \frac{x}{\Delta x} \left[\Delta T - \frac{R I_C^2}{2K} \left(\frac{x}{\Delta x} - 1 \right) \right], \quad (35)$$

$$V = V_l + \frac{x}{\Delta x} \left[\Delta V + \frac{\alpha R I_C^2}{2K} \left(\frac{x}{\Delta x} - 1 \right) \right]. \quad (36)$$

The couple of Eqs. (35-36) is in agreement with Eq. (17) that led us to the electric current in the previous section. From the temperature gradient

$$\nabla T = \frac{1}{\Delta x} \left[\Delta T - \frac{R I_C^2}{2K} \left(\frac{2x}{\Delta x} - 1 \right) \right] \frac{\mathcal{A}}{|\mathcal{A}|}, \quad (37)$$

one can, interestingly revisit the determination of I_E by multiplying Eq. (20) and inserting Eq. (37) such that

$$I_E = -K\Delta T + \left(\alpha T + V + \frac{R I_C}{2} \left(\frac{2x}{\Delta x} - 1 \right) \right) I_C. \quad (38)$$

The energy conservation across any plane with constant x , imposes that the energy current is x independent, meaning that we have exhibited a new expression of F which is a non trivial x invariant quantity within the thermoelectric material. It can be expressed in terms in term of φ as

$$F(x) \equiv \varphi(x) + \frac{R I_C}{2} \left(\frac{2x}{\Delta x} - 1 \right) = \text{Constant}. \quad (39)$$

We can thus interpret the expressions of F found in Eqs.(30) and (31) as boundary values of the invariant $F(x)$ respectively on the left and on the right side.

III. NON-EQUILIBRIUM CONDUCTANCE MATRICES

In Thermodynamic Circuit I, we use different levels of description of thermodynamic devices in view of connecting them. The fundamental level provides a non redundant basis of currents and forces [11]. The level of physical currents and forces, although linearly related, is also of interest: First, in itself to determine all the exchanges with the system's environment; second, so as to change of basis of fundamental currents. In the next section, we aim at optimizing the TEC of the former section working in different operating modes. To do so, we must provide the power of heat and work exchanges that are linearly related by the first law. This is an opportunity

for applying our framework on non-equilibrium conductance matrices for different set of currents (physical or fundamental).

In section III A, we exhibit a useful form of the selection matrix that relates physical and fundamental currents. This leads us to a specific structure (that will appear later) of the nonequilibrium conductance matrix at the level of physical currents. In section III B, we identify two sets of currents for the description of a TEC: the internal currents crossing the thermoelectric device and the external currents exchanged with the environment. In section III D, we provide the conductance matrices for fundamental, internal and external currents.

A. Structure of the conductance matrices

For self consistency, we remind below some results of Ref. [9, 11, 12] describing the selection of linearly independent currents (so-called fundamental) from a redundant set of currents (so-called physical) using conservation laws and an associated selection matrix. Then, using the current-force characteristic at the fundamental level summarized in a non-equilibrium conductance matrix, we determine a simple form of the conductance matrix at the level of physical currents. Due to a special choice of selection matrix, we find that the nonequilibrium conductance at the fundamental level is a upper left sub-matrix of the nonequilibrium conductance at the physical level.

We call \mathbf{i} the vector of physical currents and $\boldsymbol{\ell}$ the matrix whose lines are the $|\mathcal{L}|$ linearly independent conservation laws relating the $|\mathcal{P}|$ currents in \mathbf{i} . This writes in matrix form

$$\boldsymbol{\ell}\mathbf{i} = \mathbf{0}. \quad (40)$$

Note that if $\boldsymbol{\ell}$ is not full row rank, it should be reduced to a full row rank matrix by removing appropriated rows. The rank-nullity theorem states that the dimension of the kernel of $\boldsymbol{\ell}$ is $\dim(\ker(\boldsymbol{\ell})) = |\mathcal{P}| - |\mathcal{L}| = |\mathcal{S}|$. Eq. (40) thus means that

$$\mathbf{i} = \mathbf{S}\mathbf{I} \quad \text{with} \quad \boldsymbol{\ell}\mathbf{S} = \mathbf{0}, \quad (41)$$

where we have introduced the selection matrix \mathbf{S} whose columns is a possible basis of $\ker(\boldsymbol{\ell})$ and the fundamental currents vector \mathbf{I} with $|\mathcal{S}|$ components. We show in Appendix A that the selection matrix can be written as:

$$\mathbf{S} = \begin{bmatrix} \mathbb{1}_{|\mathcal{S}|} \\ \mathbf{T} \end{bmatrix}, \quad (42)$$

with $\mathbb{1}_{|\mathcal{S}|}$ the identity matrix of dimension $|\mathcal{S}|$ and \mathbf{T} a matrix that only depends on $\boldsymbol{\ell}$. The above form of selection matrix requires that the order of the components of \mathbf{i} was chosen such that

$$\mathbf{i} = \begin{pmatrix} \mathbf{I} \\ \mathbf{i}_d \end{pmatrix}. \quad (43)$$

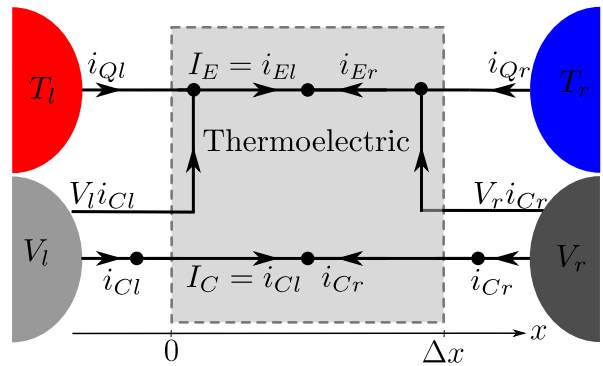


FIG. 2. The TEC is connected to two thermostats at temperature T_l and T_r with $\Delta T = T_r - T_l < 0$ and to two metallic leads at electric potentials V_l and V_r with $\Delta V = V_r - V_l > 0$. At each black dots, the Kirchoff current law can be applied. Thus at the interface with the reservoir, there exists four conservation laws. Inside the TEC, two conservation laws are available.

The vector \mathbf{i}_d of the last $|\mathcal{L}|$ components of \mathbf{i} are linear functions of \mathbf{I} . Given that the EPR is invariant under changes of level of description, it writes

$$\sigma = \mathbf{a}^T \mathbf{i} = \mathbf{A}^T \mathbf{I} \quad (44)$$

as a function of the conjugated physical force \mathbf{a} and current \mathbf{i} , or similarly of the fundamental force \mathbf{A} and current \mathbf{I} . Using Eq.(41) in Eq. (44) yields

$$\mathbf{A}^T = \mathbf{a}^T \mathbf{S} \quad (45)$$

Then, for a current-force relations reading

$$\mathbf{i} = \mathbf{g}\mathbf{a}, \quad (\text{physical level}) \quad (46)$$

$$\mathbf{I} = \mathbf{G}\mathbf{A}, \quad (\text{fundamental level}), \quad (47)$$

the nonequilibrium conductance matrices \mathbf{g} and \mathbf{G} , at respectively the physical and fundamental levels, are related by

$$\mathbf{g} = \mathbf{S}\mathbf{G}\mathbf{S}^T = \begin{bmatrix} \mathbf{G} & \mathbf{G}\mathbf{T}^T \\ \mathbf{T}\mathbf{G} & \mathbf{T}\mathbf{G}\mathbf{T}^T \end{bmatrix}. \quad (48)$$

This follows from inserting Eq. (45) and Eq. (47) in Eq. (41). Therefore, to identify the fundamental conductance matrix knowing the physical conductance matrix in a conveniently chosen basis, it suffices to read the upper left diagonal sub-matrix of dimension $|\mathcal{S}|$.

B. Physical currents and forces: external, internal

Our convention for currents is given on Fig. 2: physical currents are positive when received by the thermoelectric material in the interval $[0, \Delta x]$. Currents entering from the reservoir on the $\chi = l, r$ side (either left or right) are: the electric current $i_{C\chi}$, the heat current $i_{Q\chi}$ and

the energy current $i_{E\chi}$. The electric and energy currents of section II Eqs. (18),(29) incoming from the left are opposite to those incoming from the right:

$$i_{El} = I_E = -i_{Er} \quad (49)$$

$$i_{Cl} = I_C = -i_{Cr}. \quad (50)$$

Then, the heat current incoming from the χ side writes

$$i_{Q\chi} = i_{E\chi} - V_\chi i_{C\chi}, \quad (51)$$

Energy conservation of Eq. (49) implies that the work current received by the TEC is

$$i_W \equiv -i_{Ql} - i_{Qr} = -I_C \Delta V \quad (52)$$

The conservation laws of physical currents introduced above can be considered at the interface between the system and its environment (grey dashed line in Fig. 2) or across a plane of constant $x \in [0, \Delta x]$. To distinguish them, we call the former *external* physical currents denoted

$$\mathbf{i}_e^T \equiv (i_{Ql} \ V i_{Cl} \ i_{Cl} \ i_{Qr} \ V_r i_{Cr} \ i_{Cr}), \quad (53)$$

and the latter the *internal* physical currents denoted

$$\mathbf{i}_i^T = (i_{El} \ i_{Cl} \ i_{Er} \ i_{Cr}), \quad (54)$$

We use here indices e and i, and will do so on conjugated and fundamental variables as well. In practice, external currents are useful to make balance with the surrounding leading for instance to the received work above. The internal currents are convenient for the serial association of TECs that we will study in the next paper of this series. In any case, there is no conceptual difference between internal and external currents. For instance, one can define electric current, heat current and electric power across any transverse plane of the thermoelectric material. The conservation laws for internal currents (electric charge and energy conservation) write

$$\boldsymbol{\ell}^i \mathbf{i}_i = \mathbf{0}, \text{ with } \boldsymbol{\ell}^i = \begin{bmatrix} 1 & 0 & 1 & 0 \\ 0 & 1 & 0 & 1 \end{bmatrix}, \quad (55)$$

and those for external currents writes

$$\boldsymbol{\ell}^e \mathbf{i}_e = \mathbf{0}, \text{ with } \boldsymbol{\ell}^e = \begin{bmatrix} 1 & 1 & 0 & 1 & 1 & 0 \\ 0 & 0 & 1 & 0 & 0 & 1 \\ 0 & 1 & -V_l & 0 & 0 & 0 \\ 0 & 0 & 0 & 0 & 1 & -V_r \end{bmatrix}. \quad (56)$$

Electric charge and energy conservation are complemented by two additional conservation laws that take into account the proportionality between the ‘‘chemical’’ works $V_\chi i_\chi$ and the electric currents i_χ on each $\chi = l, r$ side. Finally, we switch between internal and external currents using

$$\mathbf{i}_i = \mathbf{P} \mathbf{i}_e, \quad \mathbf{i}_e = \mathbf{M} \mathbf{i}_i, \quad (57)$$

where

$$\mathbf{P} = \begin{bmatrix} 1 & 1 & 0 & 0 & 0 & 0 \\ 0 & 0 & 1 & 0 & 0 & 0 \\ 0 & 0 & 0 & 1 & 1 & 0 \\ 0 & 0 & 0 & 0 & 0 & 1 \end{bmatrix}, \quad \mathbf{M} = \begin{bmatrix} 1 & -V_l & 0 & 0 \\ 0 & V_l & 0 & 0 \\ 0 & 1 & 0 & 0 \\ 0 & 0 & 1 & -V_r \\ 0 & 0 & 0 & V_r \\ 0 & 0 & 0 & 1 \end{bmatrix}. \quad (58)$$

We notice that $\mathbf{P}\mathbf{M} = \mathbb{1}_4$, but $\mathbf{M}\mathbf{P} \neq \mathbb{1}_6$ even though $\mathbf{i}_e = \mathbf{M}\mathbf{P}\mathbf{i}_e$ is verified for the vector of external currents of Eq. (53). We also emphasize that, although \mathbf{P} has linearly independent lines and \mathbf{M} has linearly independent columns, one should not use their respectively right and left Moore-Penrose pseudo-inverse. This is clear for matrix \mathbf{M} that involves the electric potential which creates problems of physical dimensions when using pseudo-inverses. More importantly, and contrarily to what would come from using pseudo-inverse, matrices \mathbf{P} and \mathbf{M} provides the appropriated forces conjugated to physical currents in the EPR. Indeed, this rate is independent of the set of variables used to express it

$$\sigma = \mathbf{a}_e^T \mathbf{i}_e = \mathbf{a}_i^T \mathbf{i}_i. \quad (59)$$

In the stationary state, the EPR is

$$\sigma = - \sum_{\chi=l,r} \frac{i_{Q\chi}}{T_\chi} = - \sum_{\chi=l,r} \frac{i_{E\chi} - V_\chi i_{C\chi}}{T_\chi}. \quad (60)$$

This leads to the physical forces conjugated to internal currents

$$\mathbf{a}_i^T = \left(-\frac{1}{T_l} \ \frac{V_l}{T_l} \ -\frac{1}{T_r} \ \frac{V_r}{T_r} \right). \quad (61)$$

Using the first relation of Eq. (57) in Eq. (59) leads to the physical force conjugated to external currents

$$\mathbf{a}_e^T = \mathbf{a}_i^T \mathbf{P}, \quad (62)$$

reading explicitly

$$\mathbf{a}_e^T = \left(-\frac{1}{T_l} \ -\frac{1}{T_l} \ \frac{V_l}{T_l} \ -\frac{1}{T_r} \ -\frac{1}{T_r} \ \frac{V_r}{T_r} \right). \quad (63)$$

Now using the second relation of Eq. (57) in Eq. (59), we obtain a second relation for the forces:

$$\mathbf{a}_i^T = \mathbf{a}_e^T \mathbf{M} \quad (64)$$

which recovers Eq. (61) ensuring the consistency between the description of the TEC using internal or external currents.

C. Fundamental currents and forces: external, internal

In the previous section, we have identified the physical currents and conjugated forces (internal and external). In this section, we provide some possible fundamental

currents and forces by choosing selection matrices in the kernel of the matrix of conservation laws. We could proceed directly by inspection of the EPR, but we aim here at illustrating the general method that is convenient in more involved situations.

Let's start by choosing some fundamental currents and forces among external physical currents. There are $|\mathcal{P}_e| = 6$ linearly dependent external currents and $|\mathcal{L}_e| = 4$ associated conservation laws. We can thus choose $|\mathcal{S}_e| = |\mathcal{P}_e| - |\mathcal{L}_e| = 2$ linearly independent currents by removing $|\mathcal{L}_e| = 4$ currents from \mathbf{i}_e (one per conservation law). For instance, we can chose for fundamental currents

$$\mathbf{I}_e = \begin{pmatrix} i_{Ql} \\ V_l i_{Cl} \end{pmatrix}, \quad (65)$$

The selection matrix associated to this choice is:

$$\mathbf{S}_e = \begin{bmatrix} \mathbb{1}_2 \\ \mathbf{T}_e \end{bmatrix}, \quad \text{with } \mathbf{T}_e = \begin{bmatrix} 0 & 1/V_l \\ -1 & \Delta V/V_l \\ 0 & -V_r/V_l \\ 0 & -1/V_l \end{bmatrix}. \quad (66)$$

One can check that $\ell_e \mathbf{S}_e = \mathbf{0}$. The thermodynamic forces conjugated to the fundamental currents of Eq. (65) follows from Eq. (45)

$$\mathbf{A}_e = \begin{pmatrix} \frac{1}{T_r} - \frac{1}{T_l} \\ -\frac{1}{T_r} \frac{\Delta V}{V_l} \end{pmatrix}. \quad (67)$$

Let's continue with choosing some fundamental currents and forces among internal physical currents. There are $|\mathcal{P}_i| = 4$ linearly dependent internal currents and $|\mathcal{L}_i| = 2$ associated conservation laws. As above, we choose $|\mathcal{S}_i| = |\mathcal{P}_i| - |\mathcal{L}_i| = 2$ linearly independent currents by removing $|\mathcal{L}_i| = 2$ currents from \mathbf{i}_i (one per conservation law). For instance, we can chose for fundamental currents

$$\mathbf{I}_i = \begin{pmatrix} i_{El} \\ i_{Cl} \end{pmatrix} = \begin{pmatrix} I_E \\ I_C \end{pmatrix}. \quad (68)$$

The selection matrix associated to this choice is:

$$\mathbf{S}_i = \begin{bmatrix} \mathbb{1}_2 \\ -\mathbb{1}_2 \end{bmatrix} \quad (69)$$

We notice that \mathbf{S}_i has the structure given in Eq. (42) with $\mathbf{T}_i = -\mathbb{1}_2$. Here again, one can check that $\ell_i \mathbf{S}_i = \mathbf{0}$. The thermodynamic forces conjugated to the fundamental currents of Eq. (68) follows

$$\mathbf{A}_i = \begin{pmatrix} \frac{1}{T_r} - \frac{1}{T_l} \\ \frac{V_l}{T_l} - \frac{V_r}{T_r} \end{pmatrix} \equiv \begin{pmatrix} A_E \\ A_N \end{pmatrix}, \quad (70)$$

where we have introduced for later convenience the fundamental force A_E (respectively A_N) conjugated to energy (respectively electric) current. By construction, the EPR of the TEC is

$$\sigma = \mathbf{a}_e^T \cdot \mathbf{i}_e = \mathbf{A}_e^T \cdot \mathbf{I}_e = \mathbf{a}_i^T \cdot \mathbf{i}_i = \mathbf{A}_i^T \cdot \mathbf{I}_i. \quad (71)$$

For systems, with a small number of currents and forces, one can use the conservation laws directly in this EPR to produce a linear combination of fundamental currents only, with each linear coefficient being the conjugated force.

D. Conductance matrices for physical and fundamental variables

Eqs. (18,29) lead to a current-force characteristic in matrix form

$$\mathbf{I}_i = \begin{pmatrix} I_E \\ I_C \end{pmatrix} = -\frac{1}{R} \begin{bmatrix} \alpha F + KR & F \\ \alpha & 1 \end{bmatrix} \begin{pmatrix} \Delta T \\ \Delta V \end{pmatrix}. \quad (72)$$

This characteristic of the TEC involves a non symmetric matrix and non-conjugated currents and forces. We recover a symmetric matrix by switching to conjugated force via

$$\begin{pmatrix} \Delta T \\ \Delta V \end{pmatrix} = -\frac{T_r T_l}{\bar{T}} \begin{bmatrix} \bar{T} & 0 \\ \bar{V} & 1 \end{bmatrix} \mathbf{A}_i \quad (73)$$

yielding the current-force relation

$$\mathbf{I}_i = \mathbf{G}_i \mathbf{A}_i \quad (74)$$

with

$$\mathbf{G}_i = \frac{T_l T_r}{R \bar{T}} \begin{bmatrix} F^2 + KR \bar{T} & F \\ F & 1 \end{bmatrix}. \quad (75)$$

This conductance matrix is symmetric positive definite as required for a TEC arbitrary far from equilibrium. Since F depends on I_C , it can be expressed in terms of A_E and A_N , and so does \bar{T} . Hence, a nonequilibrium matrix provides a non-linear current-force characteristic, as expected far-from-equilibrium. We show in Appendix B, that the above conductance matrix is in principle not unique. For given mean currents, making a choice of conductance matrix amount to defining a model for quadratic fluctuations of currents [12]. We chose the form of Eq. (75) for its relative simplicity: any other form involves the supplementary definition of a bivariate function of fundamental forces. The introduction of the above nonequilibrium conductance matrices for a TEC is our first main result. It is based on the mean currents associated to the constant property model of thermoelectric [8]. Our method, applied here to thermoelectricity, provides a general way of modeling thermodynamic systems without relying on a microscopic model able to predict fluctuations at any order. The choice of a nonequilibrium conductance matrix precisely proceeds of a choice of quadratic fluctuations. We end this section by providing the conductance matrix at the physical level (external and internal) from the one at the fundamental level. First, we apply Eq. (48) using the selection matrix of Eq. (69) leading to the conductance for physical internal currents

$$\mathbf{g}_i = \mathbf{S}_i \mathbf{G}_i \mathbf{S}_i^T = \begin{bmatrix} \mathbf{G}_i & -\mathbf{G}_i \\ -\mathbf{G}_i & \mathbf{G}_i \end{bmatrix}, \quad \text{for } \mathbf{i}_i = g_i \mathbf{a}_i. \quad (76)$$

As expected this matrix is symmetric, but it is now semi-definite positive only given the linearly dependent columns and rows. Second, we use Eqs. (57,64) to write

$$i_e = \mathbf{M}i_i = \mathbf{M}g_i\mathbf{a}_i = \mathbf{M}g_i\mathbf{M}^T\mathbf{a}_e \quad (77)$$

from which one derives the conductance $\mathbf{g}_e = \mathbf{M}g_i\mathbf{M}^T$ for physical external currents. We give this conductance matrix in Table I since it can be used conveniently to extract the conductance matrix at the fundamental level for any choice of fundamental currents. To do so, one simply select \mathbf{g} 's components for the lines and columns associated to the chosen currents and forces. We remark that conjugated forces must still be determined using the appropriate selection matrix for chosen currents. As an example, one has the following current-force relation at the fundamental level

$$\begin{pmatrix} i_{Ql} \\ i_{Cl} \end{pmatrix} = \begin{bmatrix} g_{11} & g_{13} \\ g_{31} & g_{33} \end{bmatrix} \begin{pmatrix} \frac{1}{T_r} - \frac{1}{T_l} \\ -\frac{\Delta V}{T_r} \end{pmatrix}. \quad (78)$$

We use table I to read directly the conductance matrix

$$\begin{bmatrix} g_{11} & g_{13} \\ g_{31} & g_{33} \end{bmatrix} = \frac{T_l T_r}{RT} \begin{bmatrix} KR\bar{T} + (F - V_l)^2 & F - V_l \\ F - V_l & 1 \end{bmatrix} \quad (79)$$

The degree of coupling $\xi \in [-1, 1]$ between currents i_{Ql} and i_{Cl} follows

$$\xi = \frac{g_{13}}{\sqrt{g_{11}g_{33}}} = \frac{F - V_l}{\sqrt{KR\bar{T} + (F - V_l)^2}}. \quad (80)$$

It generalizes far from equilibrium the notion of degree of coupling that has a fundamental role in conversion processes [12–14].

IV. THERMODYNAMIC STUDY OF A TEC

We study now the operating modes of the TEC, their different optima (maximum power or efficiency, minimal waste) and the trade-off between power and efficiency. Our approach highlights the symmetry between the two operating modes. In section IV A, we define the partial EPRs associated to heat and work exchanges and which are relevant for the two operating modes of the TEC:

(EG) Electric Generator mode,

(HHP/CHP) Heating/Cooling Heat Pump mode,

Equations are labeled according to these acronyms to specify the operating mode they hold for. We emphasize that two utilities exist for the heat pump (cooling or heating). For all modes and utilities, we determine the range of compatible electric current. The associated device's performance can all be expressed in term of the EG's efficiency. Accordingly, for constant thermostats' temperatures and adjustable electric current, we study in section IV B the optimal working points and the power-efficiency trade-off for the EG to conclude in section IV C on the optimal working conditions of the heating or cooling HP.

A. Partial EPR, operating modes and efficiency

As is conventional, we use heat and work currents given as quadratic functions of the electric current I . Those follow directly from Eq. (29) and Eqs. (49–52):

$$i_{Ql} = -K\Delta T + \left(\alpha T_l - \frac{R}{2}I_C\right) I_C, \quad (81)$$

$$i_{Qr} = K\Delta T - \left(\alpha T_r + \frac{R}{2}I_C\right) I_C, \quad (82)$$

$$i_W = -I_C\Delta V = (\alpha\Delta T + RI_C) I_C. \quad (83)$$

To illustrate our discussion, the heat and work current are provided as a function of the dimensionless electric current $i = \frac{RI_C}{\alpha T_l}$ in the panel (A) of Fig. 3. Note that all the quantities presented in Fig. 3 are plotted versus i .

The total EPR can be decomposed into different partial EPRs pertinent for the EG and a HHP on one side $\sigma = \sigma_{Ql} + \sigma_{Wr}$, and for a CHP on another side $\sigma = \sigma_{Qr} + \sigma_{Wr}$, with

$$\sigma_{Ql} \equiv \left(\frac{1}{T_r} - \frac{1}{T_l}\right) i_{Ql}, \quad \sigma_{Wr} \equiv \frac{i_W}{T_r}, \quad (\text{HHP+EG } 84)$$

$$\sigma_{Qr} = \left(\frac{1}{T_l} - \frac{1}{T_r}\right) i_{Qr}, \quad \sigma_{Wl} \equiv \frac{i_W}{T_l}. \quad (\text{CHP } 84)$$

These partial EPRs as functions of i appear in panel (B) of Fig. 3. The TEC operates in a non trivial way when a current is opposed to its conjugated force. This is sometimes called negative response in the framework of irreversible thermodynamics [15–17]. Then, among the two partial EPRs appearing in the total EPR, one is negative and one is positive. The operating modes of the TEC are defined by

$$\sigma_{Wr} < 0 \quad \text{with} \quad \sigma_{Ql} > 0, \quad (\text{EG } 85)$$

$$\sigma_{Qr} < 0 \quad \text{with} \quad \sigma_{Wl} > 0. \quad (\text{HHP+CHP } 85)$$

This corresponds to the following intervals (shaded areas on Fig. 3) for the electric current

$$I_C \in \left] 0, -\frac{\alpha\Delta T}{R} \right[\quad (\text{EG } 86)$$

$$I_C \in]I_{C-}; I_{C+}[\quad (\text{HHP+CHP } 86)$$

where we define

$$I_{C\pm} = \frac{\alpha T_r}{R} \left(-1 \pm \sqrt{1 + \frac{2\Delta T}{ZT_r^2}} \right), \quad (87)$$

as the two electric currents for which $\sigma_{Qr} = 0$. From Eq. (87), it is clear that in our model the HP mode exists only if

$$\Delta T > -\frac{ZT_r^2}{2}, \quad (88)$$

meaning that too high temperature differences compromise the existence of a HP mode.

$$\mathbf{g}_e = \frac{T_i T_r}{R\bar{T}} \begin{bmatrix} (F - V_i)^2 + KR\bar{T} & V_i(F - V_i) & F - V_i & -((F - V_i)(F - V_r) + KR\bar{T}) & V_r(V_i - F) & V_i - F \\ V_i(F - V_i) & V_i^2 & V_i & V_i(V_r - F) & -V_i V_r & -V_i \\ F - V_i & V_i & 1 & V_r - F & -V_r & -1 \\ -((F - V_i)(F - V_r) + KR\bar{T}) & V_i(V_r - F) & V_r - F & (F - V_r)^2 + KR\bar{T} & V_r(F - V_r) & F - V_r \\ V_r(V_i - F) & -V_i V_r & -V_r & V_r(F - V_r) & V_r^2 & V_r \\ V_i - F & -V_i & -1 & F - V_r & V_r & 1 \end{bmatrix}.$$

TABLE I. Conductance matrix for physical currents and forces given in Eqs. (53) and (63).

For each operating mode and utility and following the terminology of Ref. [18], we define the type I efficiencies (or performance coefficients) as

$$\eta \equiv -\frac{i_W}{i_{Ql}} \quad (\text{EG 89})$$

$$\frac{1}{\eta} \equiv -\frac{i_{Ql}}{i_W} \quad (\text{HHP 89})$$

$$\frac{1}{\eta} - 1 \equiv +\frac{i_{Qr}}{i_W} \quad (\text{CHP 89})$$

The type II efficiencies are obtained by normalizing the type I efficiencies by their maximum value achieved for reversible conversion. We denote generically such a normalization with an overbar such that type II efficiencies write

$$\bar{\eta} = \frac{\eta}{\eta_C}, \quad \bar{\eta} = -\frac{\sigma_{Wr}}{\sigma_{Ql}}, \quad (\text{EG 90})$$

$$\frac{\bar{1}}{\eta} = \frac{\eta_C}{\eta}, \quad \frac{\bar{1}}{\eta} = -\frac{\sigma_{Ql}}{\sigma_{Wr}}, \quad (\text{HHP 90})$$

$$\frac{\bar{1}}{\eta} - 1 = \frac{\frac{1}{\eta} - 1}{\frac{1}{\eta_C} - 1}, \quad \frac{\bar{1}}{\eta} - 1 = -\frac{\sigma_{Qr}}{\sigma_{Wr}}, \quad (\text{CHP 90})$$

where we denote by $\eta_C = 1 - \frac{T_c}{T_h}$ the reversible Carnot efficiency of the EG. Type II efficiencies are also obtained as the ratio of the partial entropy production rates instead of the corresponding ratio of current as in Eq. (89). Panel (C) of Fig. 3 indicates the variation of the type II efficiencies with the dimensionless electric current i .

Finally, we introduce the ‘‘cost of energy’’

$$\text{COE} \equiv \frac{i_{Qr}}{I_C} \quad (91)$$

In the EG mode, it quantifies the amount of energy lost as heat per unit of electrical current. In the HP mode, it quantifies the amount of heat extracted from the cold reservoir per unit of the dimensionless electrical current i . The COE is given as a function of the electric current in panel (D) of Fig. 3.

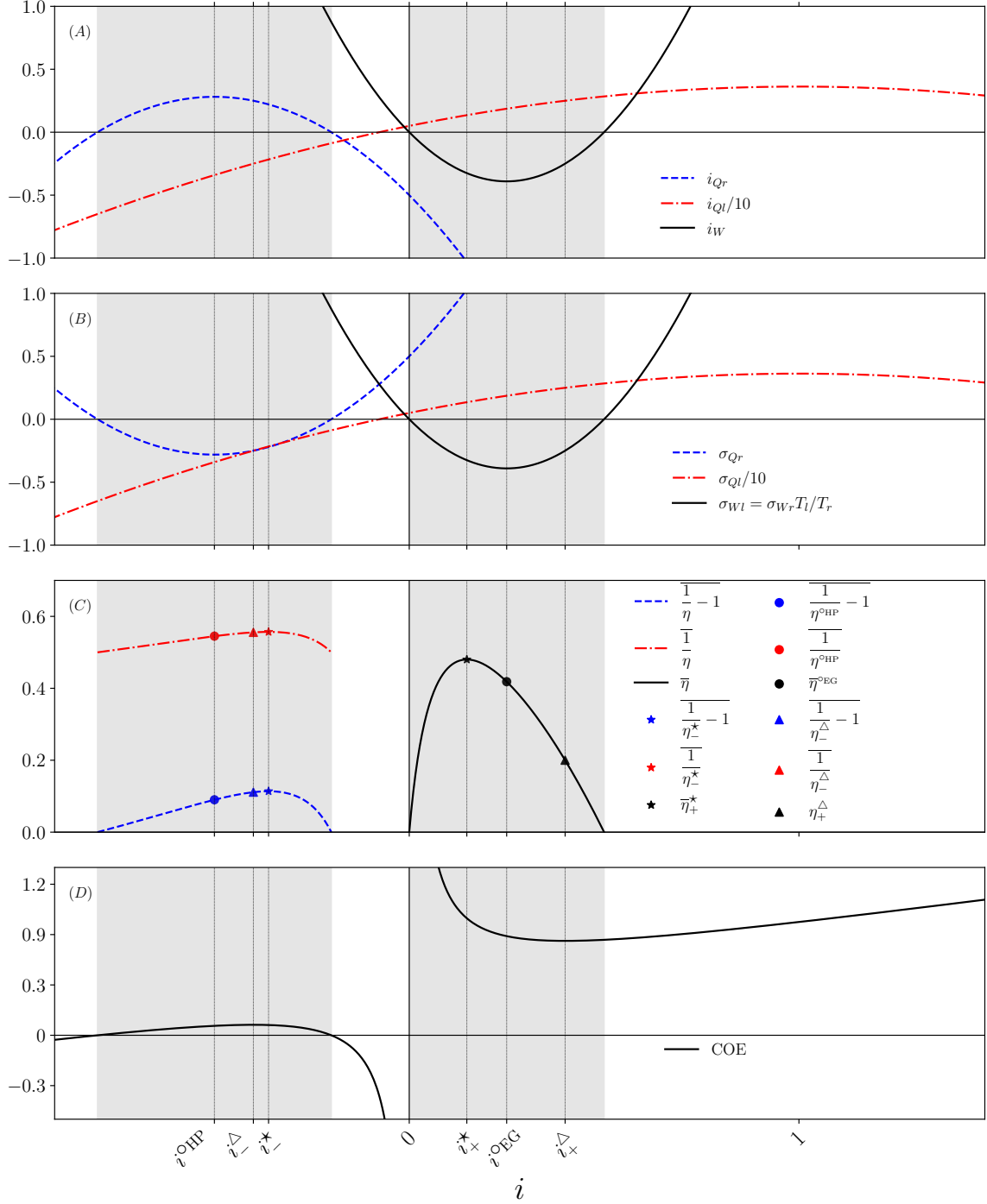


FIG. 3. (A) Incoming currents, (B) partial entropy production rates, (C) type II efficiencies and (D) cost of energy as functions of the dimensionless electric current i . The incoming currents of panel (A) are the following currents positive when received by the TEC: work (i.e. electric power) i_W (black solid line), heat incoming from the right i_{Qr} (blue dashed line) and the left i_{Ql} (red dot dashed line). The partial entropy production rates of panel (B) are associated to the currents of panel (A) with same color and line type. The type II efficiencies in panel (C) are for the CHP (blue dashed line), the HHP (red dot dashed line) and the EG (black solid line). The color and line type are the same as those for the useful current of the converter. Filled circles label the type II efficiencies and electric currents at maximum extracted heat ($y = 1$) from the right (cold) reservoir for the HP mode, and at maximum output power for the EG (i.e. of minimum i_W corresponding to $x = -1$). Filled stars label the maxima of type II efficiencies and electric currents producing those values. Filled triangles label the type II efficiencies and electric currents at the extrema of the COE. For all panels, parameters are $T_r = 1$, $T_l = 2$, $K = 1$, $R = 1$ and $\alpha = 2.5$. This unit system is defined as follows: T_r sets the temperature unit, the unit Boltzmann constant $k_B = 1$ sets the energy unit, thermal conductivity with $K T_r / (k_B T_r)$ sets the time unit, and the Seebeck coefficient α and the electric resistance R set the unit of electric current on the I axis via the ratio $2\alpha T_r / (5R) = 1$.

B. Optimal working points of the EG

We now turn to the problem of optimizing the TEC in the EG mode. We first determine the maximal efficiency, efficiency at maximum electric power and the efficiency at minimal waste at fixed ΔT (or equivalently fixed η_C). Those optima are associated respectively to stars, circles and triangles for superscript in the formula below and to the same filled symbols on Fig. 3. Then, we illustrate the power efficiency trade-off by showing that the efficiency is a bi-valued function of the electric power. We start by expressing the efficiency in terms of the following three dimensionless quantities: the Carnot efficiency η_C , the current

$$i \equiv \frac{RI}{\alpha T_l}, \quad (92)$$

and the figure of merit

$$Z\bar{T} = \frac{\alpha^2 \bar{T}}{KR}. \quad (93)$$

From Eq. (EG 89), we have:

$$\eta = \eta(i) = \frac{(\eta_C - i)i}{\frac{\eta_C(2-\eta_C)}{2Z\bar{T}} + (1 - \frac{i}{2})i}. \quad (94)$$

Optimizing the efficiency with respect to the dimensionless current i leads to the quadratic equation

$$0 = (1 - \frac{\eta_C}{2})i^2 + \frac{\eta_C(2-\eta_C)}{Z\bar{T}}i - \frac{\eta_C^2(2-\eta_C)}{2Z\bar{T}}, \quad (95)$$

whose solutions are

$$i_{\pm}^* = \frac{\eta_C}{Z\bar{T}} \left(-1 \pm \sqrt{1 + Z\bar{T}} \right) = \frac{\eta_C}{1 \pm \sqrt{1 + Z\bar{T}}} \quad (96)$$

Before simplifying $d\eta/di = 0$ into the quadratic Eq. (95), it can be used to simplify the efficiency at the optimal dimensionless current as

$$\eta_{\pm}^* \equiv \eta(i_{\pm}^*) = \frac{\eta_C - 2i_{\pm}^*}{1 - i_{\pm}^*}, \quad (97)$$

that yields with Eq. (96)

$$\bar{\eta}_{\pm}^* = \frac{\eta_{\pm}^*}{\eta_C} = \frac{-1 \pm \sqrt{1 + Z\bar{T}}}{1 - \eta_C \pm \sqrt{1 + Z\bar{T}}} \quad (98)$$

In the EG mode, the maximum efficiency is $\bar{\eta}_+^* \in [0, 1]$ obtained for the dimensionless current i_+^* . In the close-to-equilibrium limit $\eta_C \rightarrow 0$, we recover the maximum efficiency given in Eq. (85) of Ref. [19]. The limit of strong coupling ($Z\bar{T} \rightarrow \infty$) leads to the Carnot efficiency, corresponding to $\bar{\eta} \rightarrow 1$. Optimizing the output electric power (positive in EG mode)

$$-i_W = \frac{\alpha^2 T_l^2}{R} (\eta_C - i)i, \quad (99)$$

with respect to i leads to the efficiency at maximum power

$$\bar{\eta}^{\circ\text{EG}} \equiv \eta(i^{\circ\text{EG}}) = \frac{1}{\frac{1-\eta_C/2}{4Z\bar{T}} + 2 - \frac{\eta_C}{2}}, \quad \text{for } i^{\circ\text{EG}} = \eta_C/2, \quad (100)$$

associated to an output power

$$-i_W^{\circ\text{EG}} = \frac{\alpha^2 T_l^2 \eta_C^2}{4R} \quad (101)$$

The limit of strong coupling produces

$$\lim_{Z\bar{T} \rightarrow \infty} \bar{\eta}^{\circ\text{EG}} = \frac{1}{2 - \eta_C/2} \simeq \frac{1}{2} + \frac{1}{8}\eta_C + o(\eta_C), \quad (102)$$

where we made a close to equilibrium expansion in the last equality, recovering the universal expression of efficiency at maximum power [20].

For the last optimal point, we consider the cost of energy of Eq. (91) rewritten as

$$\text{COE} = -\frac{\alpha\eta_C}{Zi} - \alpha T_r - \frac{\alpha T_l}{2}i. \quad (103)$$

Its optimization with respect to i leads to the efficiency at minimal wasted heat (per unit of electric current)

$$\bar{\eta}_{\pm}^{\hat{}} = 1 - i_{\pm}^{\hat{}}/\eta_C, \quad \text{for } i_{\pm}^{\hat{}} = \pm \sqrt{\frac{\eta_C(2-\eta_C)}{Z\bar{T}}}. \quad (104)$$

Due to the positivity of the electric current in the EG mode, the optimal is for $i_+^{\hat{}}$ and the type II efficiency at minimal wasted heat is $\bar{\eta}_+^{\hat{}}$. We notice that the EG interval of current in Eq. (EG 86) write for dimensionless current $i \in [0, \eta_C]$. Hence, it can happen that there is no optimal working point with minimal wasted heat in the EG mode if $i_+^{\hat{}} > \eta_C$ (most likely for small $Z\bar{T}$). We end this section by analyzing the power efficiency trade-off in the EG mode. Since both efficiency and power are function of the electric current, one can draw the efficiency-power relation as a parametric plot. We derive below an analytical expression of efficiency as a function of the power to maximum power ratio

$$X \equiv -\frac{i_W}{i_W^{\circ\text{EG}}} = \frac{4(i - \eta_C)i}{\eta_C^2} \geq -1. \quad (105)$$

Due to our convention of positive incoming current, we preserve the fact that the dimensionless power above is negative when electric power is delivered to the outside by the TEC. The dimensionless current as a function of the power to maximum power ratio follows

$$i_{\pm} = \frac{\eta_C}{2} \chi_{\pm}, \quad \text{with } \chi_{\pm} \equiv 1 \pm \sqrt{1 + X}. \quad (106)$$

Its use in the type II efficiency gives

$$\bar{\eta} = \frac{(1 - \frac{\chi_{\pm}}{2}) \frac{\chi_{\pm}}{2}}{\frac{2-\eta_C}{2Z\bar{T}} + (1 - \frac{\chi_{\pm}\eta_C}{4}) \frac{\chi_{\pm}}{2}}, \quad (107)$$

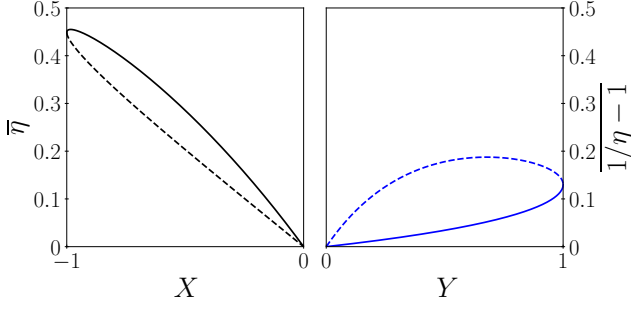


FIG. 4. Type II efficiencies $\bar{\eta}(X)$ (left panel) and $\frac{1}{\eta} - 1(Y)$ (right panel) of respectively the EG and CHP as a function of respectively X and Y , the electric and thermal power to maximum power ratios.

that is represented in the upper left panel of Fig. 4. Using i_{\pm}^* of Eq. (96) in Eq. (105), one finds that the power ratio at maximum efficiency is

$$X^* = -4 \frac{\sqrt{1 + Z\bar{T}}}{(1 + \sqrt{1 + Z\bar{T}})^2}. \quad (108)$$

C. Optimal working points of the HP

We now turn to the problem of optimizing the TEC in HP mode. The differences between the two utilities are not relevant, excepted that the heat injected in the hot reservoir has no maximum in this mode, while the extracted heat from the cold reservoir does. Given the inverse relation between the EG and HP efficiencies, we use the results of section IV B to determine the maximal efficiency, the efficiency at maximum thermal power and the efficiency at maximum COE at fixed ΔT (or equivalently fixed η_C). We keep the notations associated to those optima: stars, circles and triangles for superscript in the formula below associated to the same filled symbols on Fig. 3. Then, we illustrate the power efficiency trade-off by showing that the efficiency is a bi-valued function of the thermal power.

Optimizing the efficiency $1/\eta$ for the HHP (or $1/\eta - 1$ for the CHP) with respect to the dimensionless current i follows directly from the extrema of η for the EG. An exact computation software can show that the remaining root i_{\pm}^* of Eq. (95) belongs to the interval of electric current compatible with the HP mode:

$$\frac{RI_{C-}}{\alpha T_l} \leq i_{\pm}^* \leq \frac{RI_{C+}}{\alpha T_l} < 0 \quad (109)$$

From this dimensionless current, the efficiency η_{\pm}^* of Eq. (97), can be used to write the maximum performance coefficient of the HP (type I efficiency)

$$\frac{1}{\eta_{\pm}^*} - 1 = \frac{1 - \eta_C - i_{\pm}^*}{\eta_C - 2i_{\pm}^*}, \quad (110)$$

or after normalizing by $1/\eta_C - 1$

$$\frac{1}{\eta_{\pm}^*} - 1 = \frac{1 - \frac{\eta_C}{Z\bar{T}(1-\eta_C)}(1 + \sqrt{1 + Z\bar{T}})}{1 + \frac{2}{Z\bar{T}}(1 + \sqrt{1 + Z\bar{T}})}, \quad (111)$$

for the type II efficiency. The maximum of the output thermal power i_{Q_r} of the CHP is

$$i_{Q_r}^{\circ\text{HP}} = K\Delta T + \frac{\alpha^2 T_l^2}{2R}(1 - \eta_C)^2. \quad (112)$$

It is achieved for the optimal dimensionless current $i^{\circ\text{HP}} = \eta_C - 1$. This current used in Eq. (94) defines $\eta^{\circ\text{HP}} \equiv \eta(i^{\circ\text{HP}})$ leading to a performance coefficient at maximum thermal power (type I efficiency)

$$\frac{1}{\eta^{\circ\text{HP}}} - 1 = \frac{\eta_C(\eta_C - 2)}{2Z\bar{T}(1 - \eta_C)} + \frac{1 - \eta_C}{2} \quad (113)$$

or after normalizing by $1/\eta_C - 1$

$$\frac{1}{\eta^{\circ\text{HP}}} - 1 = \frac{\eta_C^2(\eta_C - 2)}{2Z\bar{T}(1 - \eta_C)^2} + \frac{\eta_C}{2} \quad (114)$$

for the type II efficiency. For the last optimal point, the negative current i_{\pm}^{\triangle} maximizes the COE corresponding to a maximum heat extraction from the cold reservoir per unit of electric current. This dimensionless current used in Eq. (94) defines $\eta_{\pm}^{\triangle} \equiv \eta(i_{\pm}^{\triangle})$ leading to a performance coefficient at maximum COE (type I efficiency)

$$\frac{1}{\eta_{\pm}^{\triangle}} - 1 = \frac{1}{\eta_C - i_{\pm}^{\triangle}} - 1, \quad (115)$$

or after normalizing by $1/\eta_C - 1$

$$\frac{1}{\eta_{\pm}^{\triangle}} - 1 = \frac{1 + \frac{i_{\pm}^{\triangle}}{1 - \eta_C}}{1 - \frac{i_{\pm}^{\triangle}}{\eta_C}}, \quad (116)$$

for the type II efficiency. We end this section by analyzing the power efficiency trade-off in the HP mode. The ratio of thermal power and maximum thermal power is

$$Y \equiv \frac{i_{Q_r}}{i_{Q_r}^{\circ\text{HP}}} = \frac{\eta_C + \frac{2Z\bar{T}}{2-\eta_C}(1 - \eta_C + i/2)i}{\eta_C - \frac{Z\bar{T}(1-\eta_C)^2}{2-\eta_C}} \quad (117)$$

The dimensionless current as a function of this thermal power ratio is

$$i_{\pm} = \eta_C - 1 \pm \sqrt{\frac{1 - Y}{Z\bar{T}} [(1 + Z\bar{T})\eta_C(\eta_C - 2) + Z\bar{T}]}. \quad (118)$$

We remark that i_{\pm} for $Y = 0$ leads as expected to the boundaries of the HP mode $RI_{C\pm}/(\alpha T_l)$ (for dimensionless current) and $i^{\circ\text{HP}} = \eta_C - 1$ for $Y = 1$. Using the above current as function of the thermal power to max power ratio in the type II efficiency $1/\eta - 1$ for η of Eq. (94) leads to an explicit power efficiency relation that is shown on the right panel of Fig. 4.

V. DISCUSSION AND CONCLUSION

Starting from Onsager's local description, we followed Ioffe's integrated approach, which enabled us to obtain the current-force characteristics of a TEC of finite thickness. Our derivation unraveled that within the CPM, both charge and energy flux derive from a potential. This implies that charge and energy currents follow Ohm's and Fourier's laws with appropriate resistances and potentials. We emphasize that these potentials are composite: they depend on the temperature and the electric potential. They encapsulate the coupling between charge and energy transport in thermoelectric materials. This new result will appear to be crucial in the study of thermoelectric circuits in paper III of this series. We also identified the F function, a space-invariant quantity that corresponds to the free fraction of transported energy.

We summarized the energy/matter current-force characteristics by introducing a conductance matrix relating the currents to their conjugated forces in the entropy production rate. This matrix is not unique since it corresponds to a choice of model for the coupling between matter and energy. Moreover, we gave an algebraic procedure to change the current basis using the conservation laws of the TEC. This procedure shows that two equivalent sets of currents are available for the description of a TEC: the internal currents (energy and matter), and the external currents that can be easily determined by measuring the currents (heat and matter) entering the boundaries of the TEC. For each of these current sets, we determined an associated nonequilibrium conductance matrix. In paper III of this series, we use these nonequilibrium conductance matrices to study the circuit associations of TEC in line with paper I. We emphasize that nonequilibrium conductance matrices are force-dependent and thus apply far from equilibrium.

Finally, we revisited the derivation of the optima of a TEC. We considered two non-trivial regimes accessible to the TEC: the EG and the HP mode. In both cases, a spontaneous process (with positive partial EPR) fuels a non-spontaneous process (with negative partial EPR). We clarified the study of the efficiencies in each regime by highlighting the symmetry between the EG and the HP regimes. Indeed, we have shown that the optimisation problem in each regime can be expressed in terms of the EG efficiency only. The latter presents a maximum in the EG regime and a minimum in the HP regime corresponding to maximum HP efficiency. Moreover, we introduce the cost of energy (COE) for a TEC. The latter presents an optimum for both regimes. In the case of the generator mode, it is a minimum that reflects the presence of energy consumption, even at zero charge-current. We should point out that this signature, illustrated here in the thermoelectric case, is present in all animated systems, whether living [21] or in the field of active matter [22]. Overall, this derivation of the optima of the TEC sheds light on the symmetry relating the EG regime with the HP regime.

ACKNOWLEDGMENTS

P.R. acknowledges fruitful discussions with Armand Despons.

Appendix A: Structure of the selection matrix

In this appendix, we justify the form of the selection matrix given in Eq. (42). The matrix of conservation law ℓ is of dimension $|\mathcal{L}| \times |\mathcal{S}|$ and $\text{rank}(\ell) = |\mathcal{L}|$. It describes the $|\mathcal{L}|$ linear relations between the physical currents leading to $\ell \mathbf{i} = 0$, keeping in mind that these relations are independent. Given the rank of ℓ , we can chose the order of physical currents' components of \mathbf{i} such that the $|\mathcal{L}|$ last columns of matrix ℓ , denoted ℓ_d are linearly independent. The remaining $|\mathcal{S}|$ first columns of ℓ are denoted ℓ_I . Then, we take the $|\mathcal{S}|$ first components of \mathbf{i} as our choice of fundamental currents such that

$$\mathbf{i} = \begin{pmatrix} \mathbf{I} \\ \mathbf{i}_d \end{pmatrix} \quad \text{and} \quad \ell = (\ell_I \ \ell_d). \quad (\text{A1})$$

The last $|\mathcal{L}|$ components of \mathbf{i} , denoted \mathbf{i}_d , are the dependent currents that can be obtained as linear combination of the components of \mathbf{I} . Eq. (A1) is a specific choice ensuring two properties: First, the square matrix ℓ_d has rank equal to its dimension $|\mathcal{L}|$ and hence is invertible. Second, the selection matrix relating physical and fundamental currents by $\mathbf{i} = \mathbf{S}\mathbf{I}$ writes

$$\mathbf{S} = \begin{pmatrix} \mathbb{1} \\ \mathbf{T} \end{pmatrix}, \quad (\text{A2})$$

where $\mathbb{1}$ is the identity matrix of dimension $|\mathcal{S}|$ and the matrix \mathbf{T} follows from $\ell \mathbf{S} = 0$ leading to

$$\ell_I + \ell_d \mathbf{T} = 0 \quad \Rightarrow \quad \mathbf{T} = -\ell_d^{-1} \ell_I. \quad (\text{A3})$$

This concludes our claim on the structure of the selection matrix as given in Eq. (A2).

Appendix B: Non unicity of the conductance matrices

Exhibiting a conductance matrix from the deterministic behavior, without relying on a microscopic model, cannot be done uniquely. We give an illustration of this for our model of TEC, starting from the non equilibrium conductance matrix of Eq. (75). Let's assume that there exist a matrix $\mathbf{G}'_i \neq \mathbf{G}_i$ symmetric of the form:

$$\mathbf{G}'_i = \frac{T_l T_r}{RT} \begin{bmatrix} a & b \\ b & c \end{bmatrix} \quad (\text{B1})$$

such that the fundamental current-force characteristic is preserved:

$$\mathbf{I}_i = \mathbf{G}_i \mathbf{A}_i = \mathbf{G}'_i \mathbf{A}_i, \quad (\text{B2})$$

or equivalently

$$\begin{bmatrix} KR\bar{T} + F^2 & F \\ F & 1 \end{bmatrix} \begin{pmatrix} A_E \\ A_N \end{pmatrix} = \begin{bmatrix} a & b \\ b & c \end{bmatrix} \begin{pmatrix} A_E \\ A_N \end{pmatrix}. \quad (\text{B3})$$

a system of two equations. We can solve each of them for b as function of a and c , and equalizing the results we obtain the following constraint relating a and c

$$\frac{A_E}{A_N} (KR\bar{T} + F^2 - a) = \frac{A_N}{A_E} (1 - c). \quad (\text{B4})$$

Finally, \mathbf{G}'_i can be expressed as

$$\mathbf{G}'_i = \mathbf{G}_i + \frac{T_l T_r}{RT} \begin{bmatrix} -\left(\frac{A_N}{A_E}\right)^2 & \frac{A_N}{A_E} \\ \frac{A_N}{A_E} & -1 \end{bmatrix} (1 - c) \quad (\text{B5})$$

showing that the nonequilibrium conductance matrix \mathbf{G}_i is not unique. Any value of c in the above equation pro-

duces a conductance matrix compatible with the current-force relation. We emphasize that c is in principle a function of A_E and A_N . Therefore, only its close to equilibrium value can be determined at small force when comparing the nonequilibrium conductance with Onsager's response matrix. The fact that a nonequilibrium conductance matrix includes more information on the model than the current-force relation is argued in Ref. [12]. A nonequilibrium conductance matrix can arise (with a unique definition) from a microscopic modeling. Another approach is to consider it as an alternative way of defining a model, with the idea that the additional information given on the model characterise quadratic fluctuations of currents in different nonequilibrium stationary states.

-
- [1] L. Onsager, *Phys. Rev.* **37**, 405 (1931).
[2] J. Schnakenberg, *Rev. Mod. Phys.* **48**, 571 (1976).
[3] T. L. Hill, *Free Energy Transduction and Biochemical Cycle Kinetics* (Springer-Verlag New York, Inc., 1989).
[4] L. Peusner, D. C. Mikulecky, B. Bunow, and S. R. Caplan, *The Journal of Chemical Physics* **83**, 5559 (1985), https://pubs.aip.org/aip/jcp/article-pdf/83/11/5559/18956872/5559_1_online.pdf.
[5] C. V. den Broeck and M. Esposito, *Physica A: Statistical Mechanics and its Applications* **418**, 6 (2015).
[6] A. F. Ioffe, L. S. Stil'bans, E. K. Iordanishvili, T. S. Stavitskaya, A. Gelbtuch, and G. Vineyard, *Physics Today* **12**, 42 (1959).
[7] G. J. Snyder and T. S. Ursell, *Physical Review Letters* **91**, 148301 (2003).
[8] C. Goupil, W. Seifert, K. Zabrocki, E. Müller, and G. J. Snyder, *Entropy* **13**, 1481 (2011).
[9] P. Raux, C. Goupil, and G. Verley, "Thermodynamic circuits i: Association of devices in stationary nonequilibrium," (2024), [arXiv:2309.12922 \[cond-mat.stat-mech\]](https://arxiv.org/abs/2309.12922).
[10] Y. Apertet, H. Ouerdane, C. Goupil, and P. Lecoeur, *Phys. Rev. E* **88**, 022137 (2013).
[11] M. Polettini, G. Bulnes-Cuetara, and M. Esposito, *Phys. Rev. E* **94**, 052117 (2016).
[12] H. Vroylandt, D. Lacoste, and G. Verley, *J. Stat. Mech: Theory Exp.* (2018), [10.1088/1742-5468/aaa8fe](https://doi.org/10.1088/1742-5468/aaa8fe).
[13] O. Kedem and R. S. Caplan, *Trans. Faraday Soc.* **61**, 1897 (1965).
[14] M. Polettini, G. Verley, and M. Esposito, *Phys. Rev. Lett.* **114**, 050601 (2015).
[15] B. Cleuren and C. V. den Broeck, *Europhys. Lett.* **54**, 1 (2001).
[16] P. Baerts, U. Basu, C. Maes, and S. Safaverdi, *Phys. Rev. E* **88**, 052109 (2013).
[17] G. Falasco, T. Cossetto, E. Penocchio, and M. Esposito, *New Journal of Physics* **21**, [arXiv:1812.11245 \(2019\)](https://arxiv.org/abs/1812.11245), [arXiv:1812.11245 \[cond-mat.stat-mech\]](https://arxiv.org/abs/1812.11245).
[18] A. Bejan, *Advanced Engineering Thermodynamics* (Wiley, Hoboken, NJ, 2006).
[19] C. Goupil and E. Herbert, *Entropy* **22**, 29 (2019).
[20] M. Esposito, K. Lindenberg, and C. Van den Broeck, *Phys. Rev. Lett.* **102**, 130602 (2009).
[21] C. Goupil, H. Ouerdane, E. Herbert, C. Goupil, and Y. D'angelo, *New Journal of Physics* **21**, 023021 (2019).
[22] L. K. Davis, K. Proesmans, and É. Fodor, *Physical Review X* **14**, 011012 (2024).